medRxiv

Enhancing Cognitive Performance Prediction through White Matter Hyperintensity Disconnectivity Assessment: A Multicenter Lesion Network Mapping Analysis of 3,485 Memory Clinic Patients

Marvin Petersen[1*], Mirthe Coenen[2], Charles DeCarli[3], Alberto De Luca[2,4], Ewoud van der Lelij[2], Alzheimer's Disease Neuroimaging Initiative, Frederik Barkhof[5,6], Thomas Benke[7], Christopher P. L. H. Chen[8,9], Peter Dal-Bianco[10], Anna Dewenter[11], Marco Duering[11,12], Christian Enzinger[13,14], Michael Ewers[11], Lieza G. Exalto[2], Evan F. Fletcher[3], Nicolai Franzmeier[11], Saima Hilal[9,15], Edith Hofer[16,17], Huiberdina L. Koek[2,18], Andrea B. Maier[8,9], Pauline M. Maillard[3], Cheryl R. McCreary[19], Janne M. Papma[20,21,22], Yolande A. L. Pijnenburg[23], Anna Rubinski[11], Reinhold Schmidt[16,17], Eric E. Smith[19], Rebecca M. E. Steketee[23,24], Esther van den Berg[20,21], Wiesje M. van der Flier[23,24], Vikram Venkatraghavan[23,24], Narayanaswamy Venketasubramanian[9,26], Meike W. Vernooij[20,25,27], Frank J. Wolters[25,27], Xu Xin[9,28], Andreas Horn[29,30], Kaustubh R. Patil[31,32], Simon B. Eickhoff[31,32], Götz Thomalla[1], J. Matthijs Biesbroek[2,33], Geert Jan Biessels[2], Bastian Cheng[1]

1 Department of Neurology, University Medical Center Hamburg-Eppendorf, Hamburg, Germany
2 University Medical Center Utrecht Brain Center, Utrecht, The Netherlands
3 University of California at Davis, USA
4 Image Sciences Institute, Division Imaging and Oncology, UMC Utrecht
5 Department of Radiology & Nuclear Medicine, Amsterdam UMC, Vrije Universiteit, the Netherlands
6 Queen Square Institute of Neurology and Centre for Medical Image Computing, University College London, UK
7 Clinic of Neurology, Medical University Innsbruck, Austria
8 Departments of Pharmacology and Psychological Medicine, Yong Loo Lin School of Medicine, National University of Singapore, Singapore
9 Memory, Aging and Cognition Center, National University Health System, Singapore
10 Medical University Vienna, Austria
11 Institute for Stroke and Dementia Research (ISD), LMU University Hospital, LMU Munich, Munich, Germany
12 Medical Image Analysis Center (MIAC) and Department of Biomedical Engineering, University of Basel, Basel, Switzerland
13 Division of General Neurology, Department of Neurology, Medical University Graz, Austria
14 Division of Neuroradiology, Interventional and Vascular Radiology, Department of Radiology, Medical University of Graz, Austria
15 Saw Swee Hock School of Public Health, National University of Singapore and National University Health System, Singapore
16 Division of Neurogeriatrics, Department of Neurology, Medical University of Graz, Austria
17 Institute for Medical Informatics, Statistics and Documentation, Medical University of Graz, Austria
18 Department of Geriatric Medicine, University Medical Center Utrecht, Utrecht University, Utrecht, The Netherlands
19 Department of Clinical Neurosciences and Radiology and Hotchkiss Brain Institute, University of Calgary, Calgary, Alberta, Canada
20 Alzheimer Center Erasmus MC, Erasmus MC University Medical Center, Rotterdam, The Netherlands
21 Department of Neurology, Erasmus MC University Medical Center, Rotterdam, The Netherlands
22 Department of Internal Medicine, Erasmus MC University Medical Center, Rotterdam, The Netherlands
23 Alzheimer Center Amsterdam, Department of Neurology, Amsterdam Neuroscience, Vrije Universiteit Amsterdam, Amsterdam UMC, Amsterdam, The Netherlands.
24 Amsterdam Neuroscience, Neurodegeneration, Amsterdam, The Netherlands
25 Department of Radiology & Nuclear Medicine, Erasmus MC University Medical Center, Rotterdam, The Netherlands
26 Raffles Neuroscience Center, Raffles Hospital, Singapore, Singapore
27 Department of Epidemiology, Erasmus MC University Medical Center, Rotterdam, The Netherlands.
28 School of Public Health and the Second Affiliated Hospital of School of Medicine, Zhejiang University, China
29 Charité - Universitätsmedizin Berlin, Movement Disorders and Neuromodulation Unit, Department of Neurology with Experimental Neurology, 10117 Berlin, Germany.
30 Center for Brain Circuit Therapeutics, Department of Neurology, Psychiatry, and Radiology, Brigham and Women's Hospital, Harvard Medical School, Boston, USA.
31 Institute for Systems Neuroscience, Medical Faculty, Heinrich-Heine University Düsseldorf, Düsseldorf, Germany
32 Institute of Neuroscience and Medicine, Brain and Behaviour (INM-7), Research Center Jülich, Germany
33 Department of Neurology, Diakonessenhuis Hospital, Utrecht, The Netherlands
*Correspondence should be addressed to M.P. (mar.petersen@uke.de)

Abstract. Introduction: White matter hyperintensities of presumed vascular origin (WMH) are associated with cognitive impairment and are a key imaging marker in evaluating cognitive health. However, WMH volume alone does not fully account for the extent of cognitive deficits and the mechanisms linking WMH to these deficits remain unclear. We propose that lesion network mapping (LNM), enabling the inference of brain networks disconnected by lesions, represents a promising technique for enhancing our understanding of the role of WMH in cognitive disorders. Our study employed this approach to test the following hypotheses: (1) LNM-informed markers surpass WMH volumes in predicting cognitive performance, and (2) WMH contributing to cognitive impairment map to specific brain networks. **Methods & results:** We analyzed cross-sectional data of 3,485 patients from 10 memory clinic cohorts within the Meta VCI Map Consortium, using harmonized test results in 4 cognitive domains and WMH segmentations. WMH segmentations were registered to a standard space and mapped onto existing normative structural and functional brain connectome data. We employed LNM to quantify WMH connectivity across 480 atlas-based gray and white matter regions of interest (ROI), resulting in ROI-level structural and functional LNM scores. The capacity of total and regional WMH volumes and LNM scores in predicting cognitive function was compared using ridge regression models in a nested cross-validation. LNM scores predicted performance in three cognitive domains (attention and executive function, information processing speed, and verbal memory) significantly better than WMH volumes. LNM scores did not improve prediction for language functions. ROI-level analysis revealed that higher LNM scores, representing greater disruptive effects of WMH on regional connectivity, in gray and white matter regions of the dorsal and ventral attention networks were associated with lower cognitive performance. **Conclusion:** WMH-related brain network disconnectivity significantly improves the prediction of current cognitive performance in memory clinic patients compared to WMH volume as a traditional imaging marker of cerebrovascular disease. This highlights the crucial role of network effects, particularly in attention-related brain regions, improving our understanding of vascular contributions to cognitive impairment. Moving forward, refining WMH information with connectivity data could contribute to patient-tailored therapeutic interventions and facilitate the identification of subgroups at risk of cognitive disorders.

Introduction

Cerebral small vessel disease (CSVD) is a major driver of vascular cognitive impairment (VCI) and often also contributes to dementia with a primary neurodegenerative or mixed pathology.[1] White matter hyperintensities (WMH) are the signature imaging marker of CSVD, and mark sites of white matter disintegration caused by microangiopathic axonal loss and demyelination.[2,3] However, a comprehensive understanding of mechanisms linking WMH to their broad range of clinical manifestations, specifically cognitive impairment, is still lacking.

Although there is a well-documented association between WMH volumes and cognitive functions at the group-level, the association between WMH volume and symptom severity demonstrates considerable variability with some individuals exhibiting fewer symptoms despite high WMH burden and vice versa.[4] The apparent complexity of this relationship underscores the need for improved techniques for disease quantification to more accurately predict individual cognitive impairment for effective diagnostics and ultimately targeted treatment of CSVD patients.[5] For example, lesion-symptom inference techniques have linked cognitive impairment to WMH located in strategic white matter regions, independent of total WMH volume.[4,6,7]

However, these recent findings might not fully reflect the complexity of CSVD-related cognitive impairment, which is thought to emerge from disturbances in the interplay of large-scale brain networks involving cortical and subcortical gray matter areas, interconnected by white matter tracts.[8] In recent years, advanced imaging analysis models have been developed to comprehensively capture lesion effects on brain circuitry.[9] Specifically, lesion network mapping (LNM) techniques capitalize on advanced neuroimaging to map lesions on reconstructions of the human brain network.[10] By that, a lesion's impact on connectivity to different brain regions can be quantified – i.e., the lesion's network embedding is measured – allowing to infer which regions are disconnected. Application of LNM has been shown to predict clinical symptoms in a variety of neurological disorders that can be understood as "disconnection syndromes", such as stroke or multiple sclerosis.[11,12]

Here, we propose LNM as a technique to quantify WMH-related, strategic neuronal disconnectivity for improved prediction of cognitive performance in CSVD. We employ LNM on a large-scale, multicenter dataset, integrating cognitive test results and MRI-based WMH segmentations from 3485 patients of 10 memory clinic cohorts through the Meta VCI Map Consortium.[6,13] Our hypotheses are twofold: (1) LNM-based measures of WMH disconnectivity surpass WMH volumes in predicting cognitive performance, and (2) WMH contributing to cognitive deficits map to specific brain networks that functionally determine their symptom profile.

Materials and methods

Study population

Methodological details are illustrated in *figure 1*. We examined previously harmonized, cross-sectional clinical and imaging data of 3485 patients from 10 memory clinic cohorts of the Meta VCI Map Consortium.[6,13] Meta VCI Map is a multi-site collaboration for conducting meta-analyses of strategic lesion topography in vascular cognitive impairment. The memory clinic cohorts included in this study comprise the Erasmus MC Memory Clinic Cohort (ACE, n=52, Netherlands), Alzheimer's Disease Neuroimaging Initiative (ADNI, n=994, USA)[14], UC Davis Alzheimer's Disease Center Diversity Cohort (AUCD, n=641, USA)[15], BrainIMPACT (n=53, Canada)[16], Functional Assessment of Vascular Reactivity (FAVR, n=47, Canada)[16], Harmonization (n=207, Singapore)[4], Prospective Dementia Registry (PRODEM, n=367, Austria)[17], TRACE-VCI (n=821, Netherlands)[18], Utrecht Memory Clinic Cohort (UMCC, n=227, Netherlands) and VASCAMY (n=76, Germany). All cohorts include patients assessed at outpatient memory clinics for cognitive symptoms, undergoing structural MRI alongside neuropsychological tests of cognitive performance.

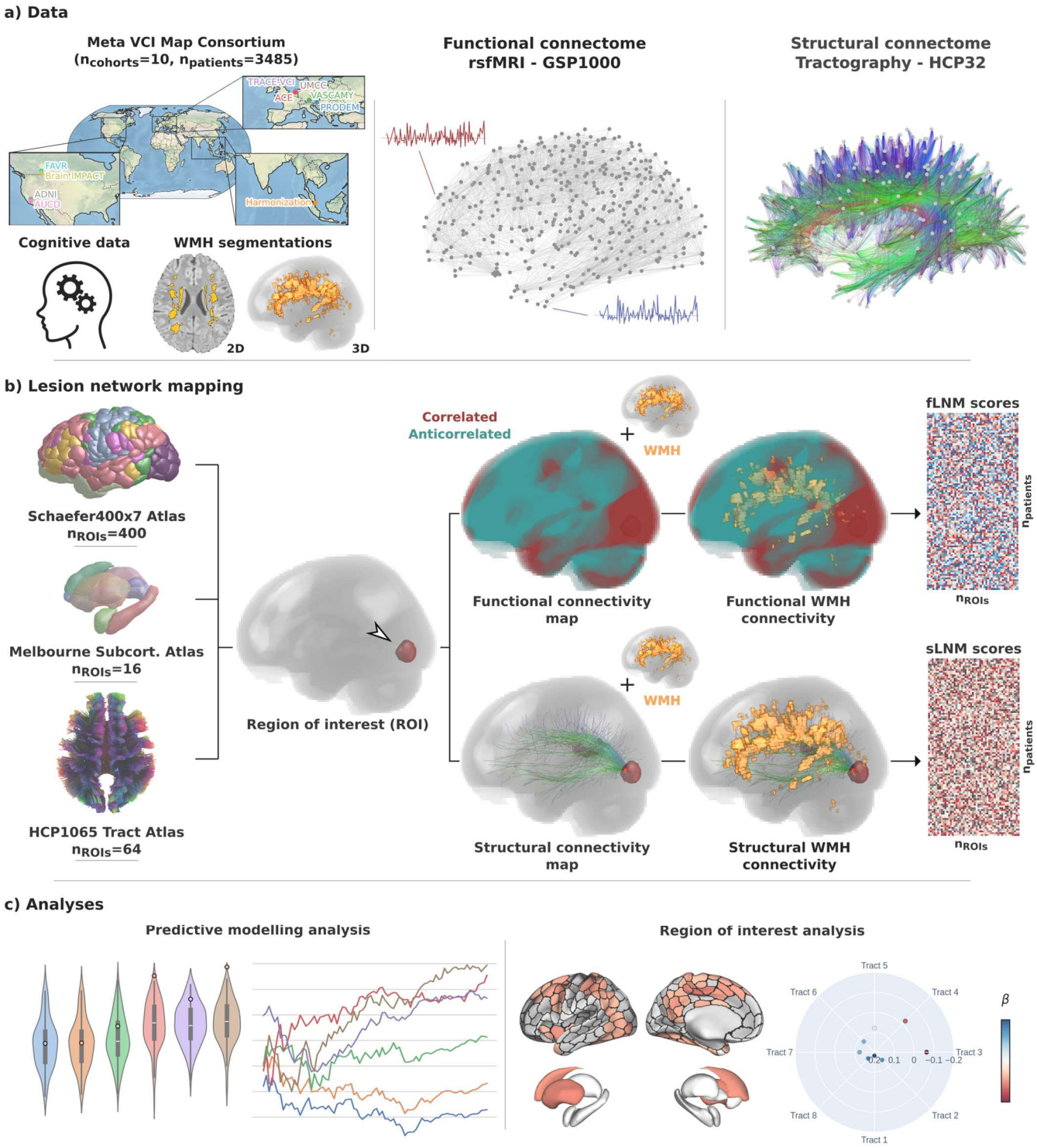

Figure 1. Methodology. a) Data from 10 memory clinic cohorts of the Meta VCI Map Consortium were used including harmonized cognitive scores and WMH segmentations in MNI space. For functional LNM we employed the GSP1000 normative functional connectome comprising resting-state fMRI data from 1000 healthy GSP participants. For structural lesion network mapping, we used the HCP32 normative structural connectome based on diffusion-weighted imaging data from 32 healthy HCP participants, detailing the fiber bundle architecture. b) LNM was performed to quantify the functional and structural connectivity of WMH to multiple ROIs (Schaefer400x7 cortical, Melbourne Subcortical Atlas subcortical, HCP1065 white matter areas). For this, voxel-level functional and structural connectivity maps were computed for each ROI, reflecting resting-state BOLD correlations or anatomical connection strength via tractography streamlines, respectively. ROIwise LNM scores were derived by averaging voxel-level connectivity indices within the normalized WMH masks, considering only positive correlation coefficients for functional mapping. This resulted in a matrix for both fLNM and sLNM scores per ROI per patient (n_{ROIs} x $n_{patients}$). The matrices shown in the figure are populated with random data only serving as a visual aid. c) The fLNM and sLNM scores across patients were used in predictive models to estimate cognitive domain scores (predictive modelling analysis) and analyzed in permutation-based general linear models to identify regions significantly influencing the cognitive domain-WMH disconnectivity relationship at the ROI level (ROI-level inferential statistics). *Abbreviations*: fLNM = functional lesion network mapping, GSP = Genomic Superstruct Project, HCP = Human Connectome Project, ROI = region of interest, rsfMRI = resting-state functional magnetic resonance imaging, sLNM = structural lesion network mapping, WMH = white matter hyperintensities of presumed vascular origin.

Patients with cognitive impairment due to non-vascular, non-neurodegenerative causes (e.g., excessive alcohol use disorder, cerebral malignancies, multiple sclerosis) or monogenic disorders (e.g., CADASIL) were excluded. Further details on each cohort including sample-specific inclusion and exclusion criteria were reported previously.[6]

Ethics approval

All cohorts received the requisite ethical and institutional approval in accordance with local regulations, which included informed consent, to allow data acquisition and sharing.[6]

Cognitive assessments

Detailed harmonization procedures, including specific test-to-domain assignments, were reported previously.[19] Neuropsychological tests from participating cohorts were norm-referenced against local norms or a healthy control group, and adjusted on the individual subject level for age, sex, and education. These tests were categorized into four cognitive domains: attention/executive function, information processing speed, language, and verbal memory. Within these domains, norm-referenced neuropsychological test scores were z-scored and averaged to obtain cognitive domain scores (z-scores), which capture individual-level cognitive domain performance relative to healthy controls.

White matter hyperintensity segmentation

WMH segmentations were provided by the participating centers, or performed at the UMC Utrecht (ACE cohort). Segmentation masks were obtained applying established automated neuroimaging software on fluid-attenuated inversion recovery (FLAIR) MRI.[20] WMH segmentations were spatially normalized to the Montreal Neurological Institute (MNI)-152 template.[21] To ensure registration quality, the normalized WMH masks were visually inspected and patients with failed registrations were excluded. Furthermore, random subsamples of normalized WMH segmentations were returned to the respective participating institutions to confirm the data quality. WMH segmentation masks were used to compute the total WMH volume as well as tract-level WMH volumes for each of the 64 white matter fiber tracts of the HCP1065 Tract Atlas.[22] Details on cohort-specific segmentation and registration procedures were reported previously.[6,23]

Lesion network mapping

LNM was performed to quantify the functional and structural connectivity of WMH to cortical, subcortical and white matter regions of interest (ROIs).[24] ROIs were defined in MNI space according to the Schaefer400x7 Atlas (n_{ROIs}=400), the Melbourne Subcortical Atlas (n_{ROIs}=16) and the HCP1065 Tract Atlas (n_{ROIs}=64) (*figure 1b*).[22,25,26] For visualization of the investigated HCP1065 tracts, see *supplementary figure S1*.

Functional lesion network mapping (fLNM) was conducted using a normative functional connectome, derived from resting-state fMRI scans of 1,000 healthy individuals from the Genomic Superstruct Project (GSP1000).[27] Preprocessing included global signal regression and spatial smoothing at a 6mm full width at half maximum kernel as previously detailed.[28] For each ROI, we averaged blood oxygen level-dependent (BOLD) signal fluctuations across voxels within the ROI and correlated this aggregate time series with BOLD signals of all brain voxels. This process generated 1,000 Pearson correlation coefficients per voxel, i.e., one for each GSP1000 subject, which were then Fischer z-transformed and averaged across subjects to create a functional connectivity map per ROI. Functional connectivity map computations were performed using the ROI masks as seeds in the *connectome mapper* function of Lead-DBS (lead-dbs.org).[29] Subsequently, ROI-level fLNM scores were calculated by averaging positive Pearson correlation coefficients within the WMH mask, reflecting each ROI's functional connectivity to WMH.

Structural lesion network mapping (sLNM) was performed employing a normative structural connectome of 32 subjects of the Human Connectome Project (HCP32).[30] The structural connectome was reconstructed by applying DSI Studio on multi-shell diffusion MRI data acquired on a MRI scanner specifically designed for high-fidelity connectome reconstruction. Streamlines resulting from whole brain tractography were normalized to MNI and aggregated across subjects.[31] Employing Lead-DBS, voxel-wise structural connectivity maps were computed per atlas ROI, quantifying per voxel the number of streamlines connecting the voxel to the ROI.[29] ROI-level sLNM scores, reflecting structural connectivity between WMH and individual ROI, were determined by averaging the voxel values (representing streamline counts to the ROI) within the WMH mask.

Summarized, LNM yielded both a fLNM and sLNM score for each ROI per subject, indicating the functional and structural connectivity between WMH and ROI, respectively.

Predictive modelling analysis

To evaluate the predictive capacity of fLNM and sLNM scores, we performed a predictive modelling analysis leveraging scikit-learn (v. 1.0.2, scikit-learn.org) and julearn (v. 0.3.0, juaml.github.io/julearn).[32,33] In the analysis, six different feature sets were compared: (1) confounds (age, sex and education), (2) total WMH volume + confounds, (3) tract-level WMH volumes + confounds, (4) ROI-level fLNM scores + confounds, (5) ROI-level sLNM scores + confounds, (6) ROI-level fLNM and sLNM scores + confounds.

For each cognitive domain, multivariable ridge regression models were trained using the abovementioned feature sets to predict cognitive domain scores. Ridge regression models include a L2 penalty that reduces coefficients to mitigate overfitting and address multicollinearity. We optimized the L2 penalties through a 10-fold nested cross-validation, tuning α values ranging from 0.001 to 1000 (α = 0.001, 0.01, 0.1, 1, 10, 100, 1000). The model performance was scored by the Pearson correlation between actual and predicted cognitive domain scores, supplemented with explained variance (R^2, coefficient of determination) and negative mean squared error as additional measures of performance. In line with best practices, explained variance was calculated via sum-

of-squares formulation (using scikit-learn's *r2_score*) instead of squaring Pearson correlations.[34] Before model fitting, continuous input features were z-scored in a cross-validation consistent manner to avoid data leakage.[35] To maintain a consistent distribution of the target variable across training and test sets, we employed julearn's *ContinuousStratifiedKFold* function for creating the folds. Cross-validations were repeated 10 times with varied random splits to minimize bias from any single split.[36] This approach yielded 100 scores for each feature-target set combination which were compared between feature sets using a machine learning-adjusted t-test.[37] We repeated the predictive modelling analysis for different sample sizes (20%-100%, 1% steps, randomly sampled) to examine the robustness and sample size dependency of predictive performances. As a whole, this analysis follows current best practices of predictive modelling in neuroimaging.[34]

Region of interest-level inferential statistics

To investigate whether WMH-related disconnectivity of specific brain circuits links to impaired cognitive performance, we conducted permutation-based testing for linear associations between regional LNM scores and cognitive domain scores in a general linear model. All statistical analyses were conducted in FSL's Permutation Analysis of Linear Models (PALM) based on MATLAB (v. 2021b) and Python 3.9.1 leveraging neuromaps (v. 0.0.5).[38–40] Statistical tests were two-sided ($n_{permutation}$=5000), with a $p<0.05$ as the significance threshold. To account for multiple comparisons, p-values were adjusted for family-wise error. General linear models were adjusted for age, sex and education. To obtain standardized β-coefficients, input variables were z-scored beforehand. As a result, β-coefficients and p-values were obtained for each cortical, subcortical, and white matter ROI (n_{ROIs}=480) indicating the strength and significance of the LNM score's linear association with cognitive domain scores for each ROI. To aid in interpreting the spatial effect patterns, we averaged the β-coefficients representing cortical effects in the 7 intrinsic resting-state networks (Yeo networks), which reflect the cerebral cortex's intrinsic functional organization.[28] The Schaefer400x7 Atlas assigns ROIs to these networks: visual, somatomotor, dorsal attention, ventral attention (salience), limbic, frontoparietal control, and default mode network.[25] Significance was tested via spin permutations (n_{spins}=1000) which represent a null model preserving the inherent spatial autocorrelation of cortical information.

Sensitivity analyses

During computations of fLNM scores, we decided to only consider positive Pearson correlations of resting-state BOLD signal within WMH masks following previous approaches as the role of negative correlations is controversial.[41] However, some studies suggest biological meaning in anticorrelations of BOLD signal fluctuations.[42,43] Hence, we conducted a sensitivity analysis based on fLNM scores computed by averaging only the negative Pearson correlations in the WMH masks. We reconducted the predictive modelling analysis and ROI-level inferential statistics using these negative fLNM scores.

Moreover, previous work employs thresholding to discard potentially noisy connectivity information. To further examine the effect of thresholding on our results we repeated the predictive modelling analysis comparing the main analysis results to fLNM and sLNM scores computed based on 25% and 50% highest voxel intensities in the WMH mask. For negative fLNM scores, the lowest 25% and 50% voxel intensities in the WMH mask were considered.

Exploratory analyses

Further exploratory analyses including investigations of voxel-level lesion network maps and structure-function coupling of LNM scores are described in *supplementary text S2.*

Data availability

Analysis code can be accessed on GitHub (https://github.com/csi-hamburg/2024_petersen_wmh_disconnectivity_memory_clinic). The data that support the findings of this study are available from the corresponding author/project leads on reasonable request (https://metavcimap.org/group/become-a-member/). Restrictions related to privacy and personal data sharing regulations and informed consent may apply.

Results

Sample characteristics

The pooled study sample of 3485 patients had a mean age of 71.7 ± 8.9 years and 49.8% were female. Among patients, 777 (22.3%) had subjective cognitive impairment, 1389 (39.9%) had mild cognitive impairment, and 1319 (37.9%) had dementia. Further details on the sample characteristics can be found in *table 1*. A heatmap of WMH distribution can be found in *supplementary figure S3.*

Predictive modelling analysis

To evaluate if information on WMH network connectivity exceeds the predictive capacity of volumetric WMH metrics for cognitive performance, we first computed regional fLNM and sLNM scores, that capture the structural and functional disconnection induced by WMH. We then employed ridge regression for predictive modelling. Model performance was assessed via Pearson correlation (r) of predicted and actual cognitive domain scores averaged across folds. All models incorporated age, sex, and education (confounds) as features to establish a performance baseline. The corresponding results are visualized in *figure 2a*. In summary, LNM scores significantly improved cognitive function prediction in all domains, except language, over WMH volumes. In detail, the predictive performance achieved by the confounds-only model was r = 0.312 for attention / executive function, r = 0.239 for information processing speed, r = 0.404 for language, and r = 0.305 for verbal memory. Models informed by total or tract-wise WMH volumes achieved a predictive performance of r = 0.341 - 0.365 for attention / executive function, r = 0.247 – 0.250 for information processing speed, r = 0.404 – 0.416 for language, and r = 0.327 – 0.356 for verbal memory. For the prediction of attention / executive function, models

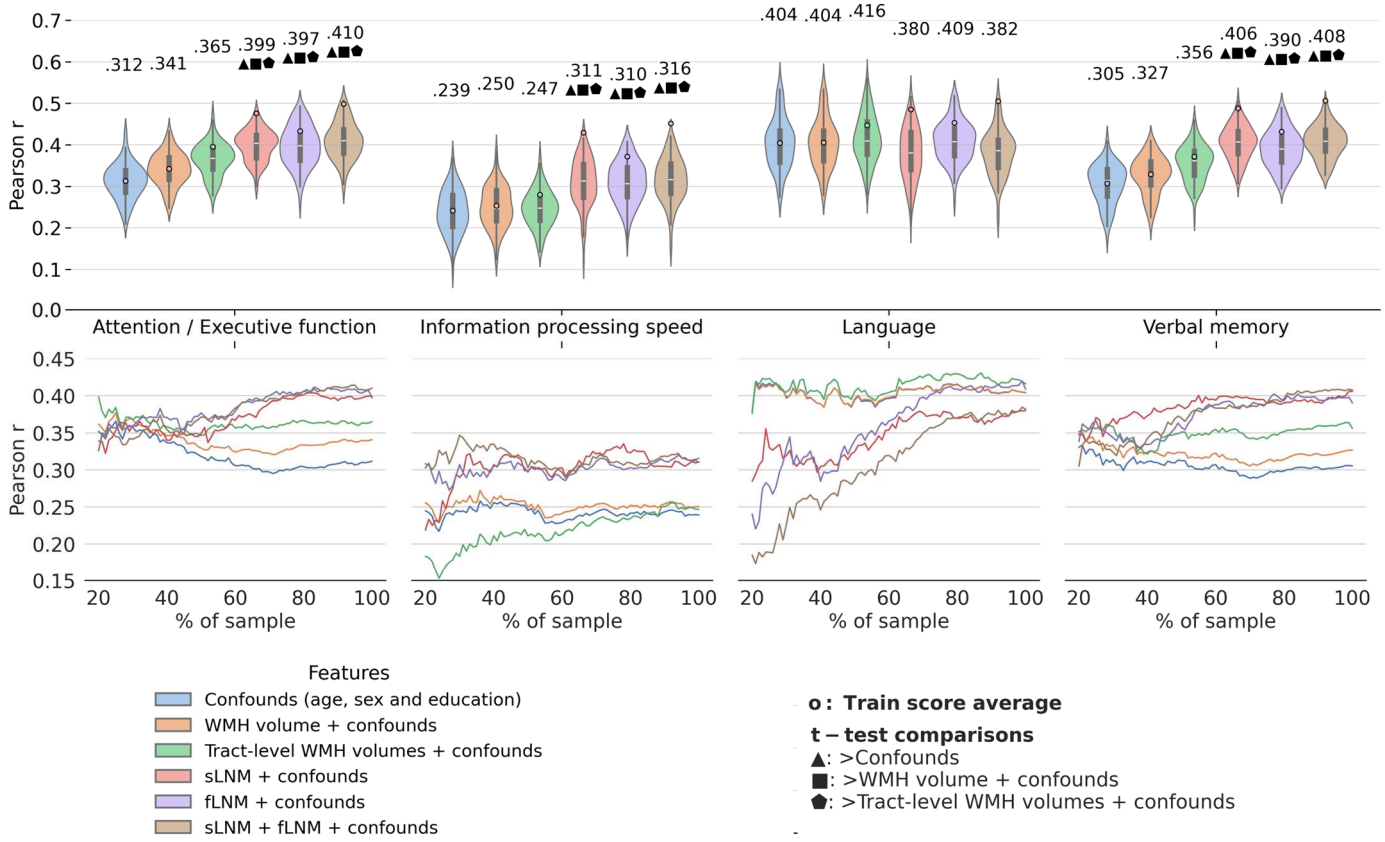

Figure 2. Predictive modelling analysis. Violin plots illustrate prediction outcomes across cognitive domains. Each violin displays the distribution of Pearson correlations (between actual and predicted cognitive domain performance; 10-fold cross-validation × 10 repeats = 100 folds → 100 Pearson correlations) for a model informed by a different feature set. The higher the Pearson correlation, the higher the prediction performance. blue: confounds (age, sex and education); orange: total WMH volume + confounds; green: tract-level WMH volumes + confounds; red: sLNM scores + confounds; purple: fLNM scores + confounds; brown: sLNM scores + fLNM scores + confounds. Average Pearson correlations are indicated above each violin, with colored dots showing training score averages. Geometric symbols denote t-test results comparing LNM-based models against confound- and WMH volume-based models: ▲ indicates higher Pearson correlation than confounds, ■ than WMH volume + confounds, ⬟ than tract-level WMH volume + confounds. Below the violin plots, performance curves display the average Pearson correlations across folds, for subsets randomly sampled in sizes ranging from 20% to 100% of the entire dataset. Line colors match the corresponding violin plots in panel a) which display predictive modelling results for the full sample size. Again, higher Pearson correlation indicates higher prediction performance. *Abbreviations*: fLNM = functional lesion network mapping, sLNM = structural lesion network mapping, WMH = white matter hyperintensities of presumed vascular origin.

informed by LNM scores exhibited a significantly higher predictive performance than models informed by volumetric WMH measures (LNM: r = 0.399 - 0.410 vs. WMH volume: r = 0.341 – 0.365; adjusted t-test, all $p < 0.05$). LNM-informed models also better predicted information processing speed (LNM: r = 0.310 - 0.316 vs. WMH volume: r = 0.247 – 0.250, adjusted t-test, all $p < 0.05$) as well as verbal memory (LNM: r = 0.390 - 0.408 vs. WMH volume: r = 0.327 – 0.356; adjusted t-test, all $p < 0.05$). Across these domains, the best prediction was achieved by models incorporating both structural and functional LNM scores. For attention / executive function, comparing the improvement from the confounds-based model to the model informed by total WMH volume (0.341 – 0.312 = 0.029) with the improvement to the model based on both LNM modalities (0.410 – 0.312 = 0.098), the usage of fLNM and sLNM scores amounts to a 3.38-fold increase (0.098 / 0.029 = 3.38) in added predictive performance. Considering both LNM modalities for predicting information processing speed and verbal memory amounted to 7.00-fold and 4.68-fold increase in predictive performance, respectively. For the prediction of language domain scores, performance between LNM-informed models and WMH volume measures did not differ significantly (LNM: r = 0.380 - 0.409 vs. WMH volume: r = 0.404 – 0.416, all $p > 0.05$). See *supplementary materials S4* and *S5* for predictive modelling results using explained variance and negative mean squared error as scoring methods. Details on regional averages of LNM scores are shown *supplementary figure S6*.

To test the robustness of prediction results, we repeated the analysis in randomly chosen subsamples of increasing sizes (*figure 2b*). For attention / executive function and verbal memory, LNM-informed models started to consistently exceed WMH volume-based models at approximately 50% (attention / executive function: n=1723, verbal memory: n=1712; note that data availability differed between cognitive domain scores) of the sample size. For information processing speed, LNM-informed models surpassed WMH volume-based models at approximately 25% (n=604) of the sample size. Regarding language, LNM-informed models approximated the performance of WMH volume-based models with increasing sample sizes. For all cognitive domain scores, predictive performance in the sample size range 80-100% showed high stability and only minor increases indicating saturation.

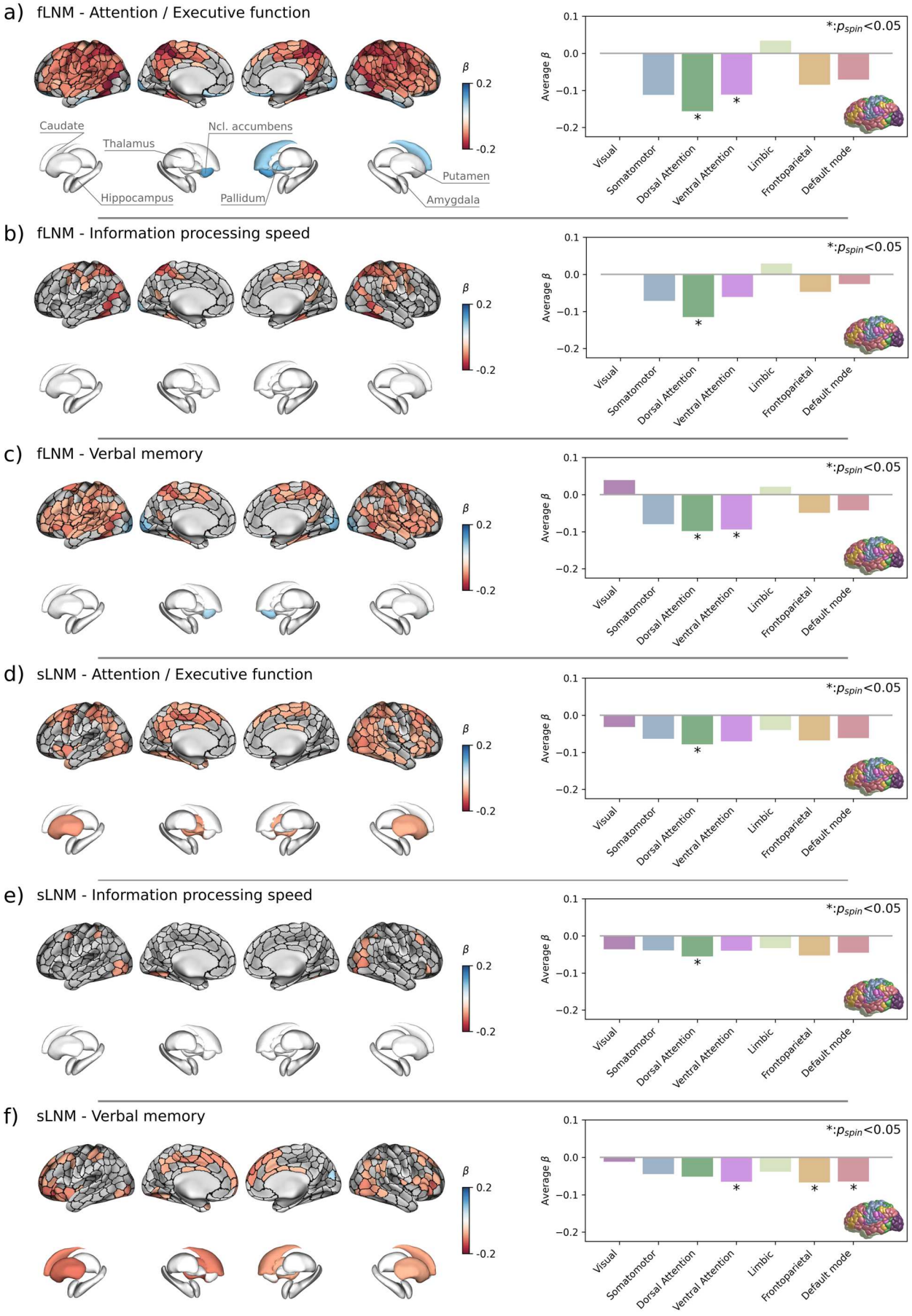

Figure 3. Inferential statistics results of cortical and subcortical gray matter. Anatomical plots on the left side display the regional relationship between LNM scores and cognitive domain scores. ROIs in which LNM scores across participants were significantly associated with cognitive domain scores after family-wise error-correction are highlighted by colors encoding β-coefficients from general linear models: a negative β (red) denotes that a higher regional LNM score, i.e., higher WMH disconnectivity, is associated to a lower performance in individual cognitive domains; a positive β (blue) indicates that a higher regional LNM score is linked to a higher cognitive domain performance. Barplots on the right side display the corresponding β coefficients averaged in the canonical (Yeo) resting-state functional connectivity networks. The brain in the lower right corner indicates the regional distribution of the canonical resting-state networks with colors corresponding to the bars. Statistical significance was assessed using spin permutations. Each row corresponds with a different combination of lesion network mapping modality and cognitive domain: a) fLNM – attention / executive function, b) fLNM – information processing speed, c) fLNM – verbal memory, d) sLNM – attention / executive function, e) sLNM – information processing speed, f) sLNM – verbal memory. *Abbreviations*: fLNM = functional lesion network mapping, p_{spin} = p-value derived from spin permutations, ROIs = regions of interest, sLNM = structural lesion network mapping.

Contextualization of WMH disconnectivity: Region of interest analysis

We tested if WMH disconnectivity of specific brain circuits links to cognitive performance by quantifying the association between *regional* LNM scores (cortical brain regions and white matter tracts) and cognitive domain scores adjusting for age, sex and education.

Results of the general linear model linking LNM scores in cortical and subcortical gray matter regions to cognitive domain scores are shown in *figure 3*. Higher fLNM scores (i. e. increased WMH-related disconnection) in cortical regions of the dorsal attention and ventral attention networks were linked to lower attention / executive function and verbal memory (*figure 3a* and *c*). Regarding information processing speed, the extent of the effect was limited to several cortical brain areas mapping to the dorsal attention network (*figure 3b*). In terms of sLNM, higher scores in the dorsal attention network were significantly associated with lower attention / executive function and information processing speed (*figure 3d* and *e*). Again, information processing speed showed a spatially more limited effect pattern. The relationship of regional sLNM and verbal memory scores showed a different spatial distribution mapping to the ventral attention, frontoparietal and default mode network (*figure 3f*). The cortical and subcortical LNM scores showed no significant association with the language domain score.

The results for anatomically predefined white matter tracts are shown in *figure* 4. For tract-level fLNM, lower cognitive performance in attention / executive function, information processing speed and verbal memory was most strongly linked to higher fLNM scores in association and projection tracts connecting the parietal cortex (*figure 4b*): the middle longitudinal fasciculus (MdLF), parietal corticopontine tract (CPT), dorsal, medial and ventral sections of the superior longitudinal fasciculus (SLF 1-3), the parietoparahippocampal cingulate (C parietoparahipp.). For attention / executive function, a strong negative effect was also evident for the right arcuate fasciculus (AF). For verbal memory, significant negative effects were additionally found for the corticobulbar tract (CBT) and frontal aslant tract (FAT).

Regarding tract-level sLNM, lower attention / executive function and verbal memory were significantly associated with higher sLNM scores in association and projection tracts connecting frontal regions (*figure 4c*): the frontoparahippocampal cingulate (C parietoparahipp.), parolfactory cingulate (C parolfactory), the superior longitudinal fasciculus (SLF 1-3), frontoparietal cingulate (C frontoparietal), anterior thalamic radiation, anterior corticostriatal pathways (CS anterior), uncinate fascicle, frontal corticopontine tract (CPT frontal). For attention / executive function, a strong negative effect was also evident for the right arcuate fasciculus (AF). Furthermore, higher verbal memory scores were significantly linked to higher sLNM scores in the fornices. Information processing speed showed a significant negative association with sLNM scores in the right medial superior longitudinal fasciculus (SLF 2) and frontoparahippocampal cingulate (C frontoparahipp.). Tract-level LNM scores showed no significant association with language function. For plots displaying all tract-level associations refer to *supplementary figures S7* and *S8*.

The spatial effect patterns, i.e., β-coefficient maps, showed significant overlap with 26 of 28 effect pattern pairs being significantly correlated (see *supplementary figure S9* for a correlation matrix).

Sensitivity analyses

Predictive modelling results were stable when using negative fLNM scores (based on anti-correlations in resting-state fMRI measures) and when including a 25% or 50% thresholding step (*supplementary figure S10*). Exploratory ROI-level inferential statistics based on negative fLNM scores indicated that lower attention / executive function and information processing speed were more significantly associated with more negative fLNM scores in the default mode network (*supplementary figure S11 & S12*).

Exploratory analyses

Exploratory analyses are detailed in *supplementary text S2*. Functional and structural LNM scores were significantly correlated across ROIs and across subjects (*supplementary figure S13*). Voxel-level lesion network maps indicating white matter regions that contribute to variance in cognitive domain function are shown in *supplementary figure S14 & S15*.

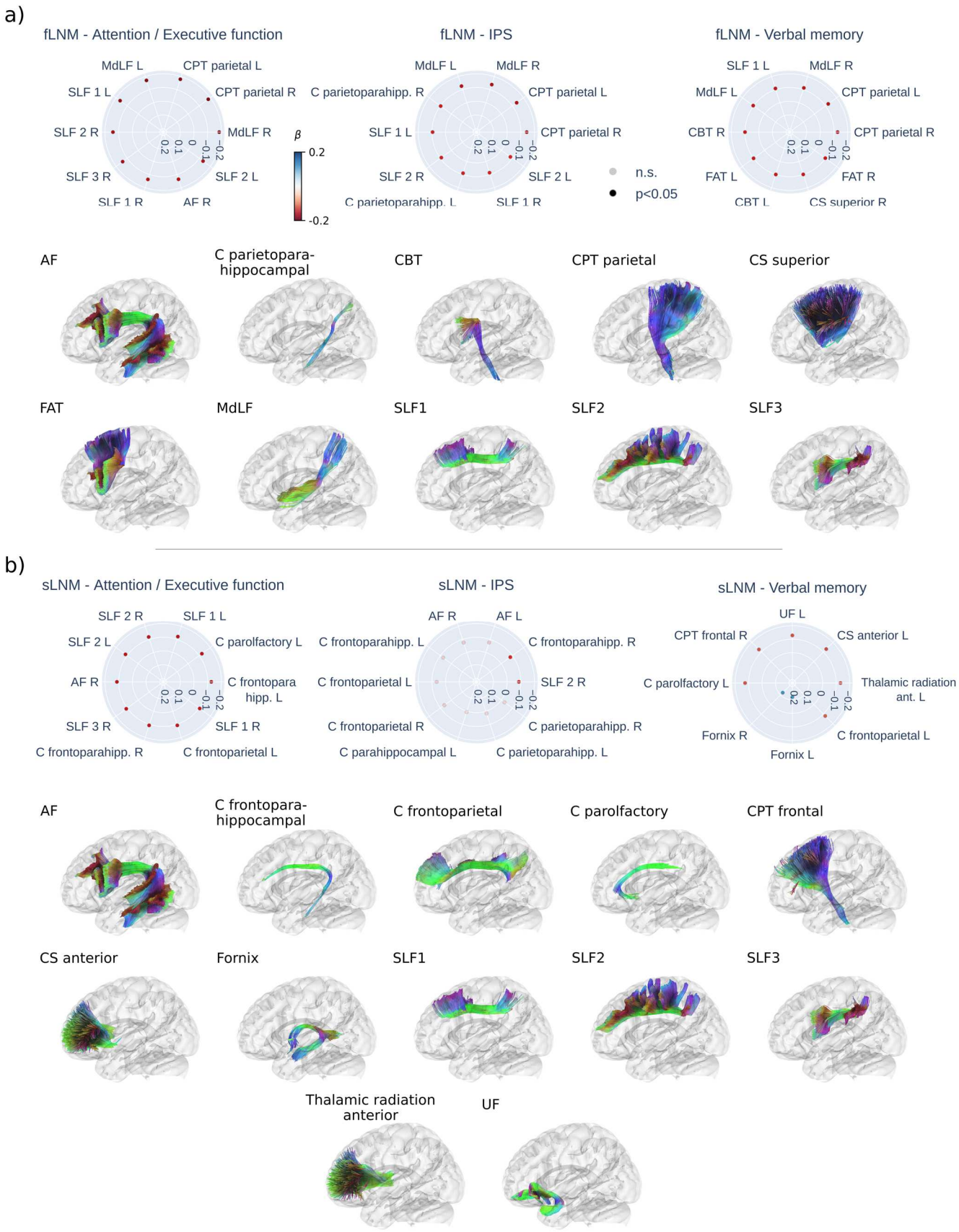

Figure 4. Inferential statistics results of white matter tracts. Radar plots displaying the top 10 of strongest linear associations (standardized β) for the functional (a) and structural (b) lesion network mapping scores in each tract in association with cognitive domain scores. Strongest associations are shown at the 3 o'clock position, decreasing in strength counterclockwise. Red dots indicate a negative association (higher LNM score – lower cognitive domain score) and blue dots indicate a positive association (higher LNM score – higher cognitive domain score). Faintly colored dots indicate non-significant associations. Tracts with a significant association are displayed below the radar plots in alphabetical order. For paired tracts only left side examples are visualized. *Tract abbreviations*: AF = arcuate fascicle, C = cingulate, CBT = corticobulbar tract, CPT = corticopontine tract, CS = corticostriatal pathway, F = fornix, FAT = frontal aslant tract, MdLF = middle longitudinal fasciculus, SLF = superior longitudinal fasciculus, UF = uncinate fasciculus; *Abbreviations*: fLNM = functional lesion network mapping, IPS – information processing speed, n.s. = non-significant, p = p-value, sLNM = structural lesion network mapping.

Discussion

In a large multicentric sample of memory clinic patients, we conducted an in-depth examination of the link between functional and structural LNM scores and cognitive performance. We report two main findings: (1) both structural and functional LNM scores, capturing WMH-related disconnectivity, significantly improved the prediction of cognitive performance compared to WMH volume; (2) WMH-related disconnectivity associated with lower cognitive performance, predominantly affected the dorsal and ventral attention networks.

LNM scores surpass WMH volumes in predicting cognitive performance

In current clinical practice, vascular cognitive impairment in individual patients is often attributed to total WMH burden, but interindividual variance in this relationship can lead to diagnostic dilemmas. Previous research has demonstrated that strategic WMH locations, specifically in commissural and association tracts are statistically more likely to be associated with lower cognitive performance.[4,6,7] Our approach adds to this perspective, not only considering the localization of WMH but also integrating them with network connectivity information to capture the WMH network embedding. In our analysis, statistical models capitalizing on LNM scores demonstrated superior performance over those relying on total or tract-level WMH volume in predicting cognitive performance in almost all cognitive domains. As this analysis implements current best practices of predictive modelling in neuroimaging, our findings represent evidence for a true prediction of cognitive performance by LNM.[34] Comparing the improvement from the confounds-based model to the model informed by total WMH volume with the improvement to the model based on both LNM modalities, the usage of fLNM and sLNM scores yielded to a 3- to 7-fold increase in added predictive performance across the three cognitive domains. Moreover, our findings highlighted that total WMH volumes only marginally surpass age, sex, and education in predictive accuracy, stressing the importance of including demographic confounds as baselines in predictive models involving WMH volume. Collectively, these findings are important, given the longstanding reliance on WMH extent as a primary imaging surrogate marker for cognitive impairment in CSVD. We provide evidence for the considerable role of WMH-related "covert" network effects as indicated previously in studies from smaller clinical or population-based studies.[8,44–46]

Improved prediction of cognitive performance was achieved irrespective of the applied LNM modality. Contrasting prior studies suggesting the inferiority of functional LNM compared to structural approaches for predicting cognitive performance post-stroke,[9,47] our contrary findings might arise from differences in the LNM approach as well as our focus on WMH rather than ischemic stroke lesions. The ROI-based functional LNM method we used may be more suitable to detect the widespread network disturbances induced by WMH, as opposed to the localized disruptions from stroke lesions. Notably, fLNM and sLNM scores were positively correlated, suggesting some degree of structure-function coupling that could account for their comparable predictive performance. However, the correlation strength was mostly moderate and prediction performance of fLNM and sLNM differed noticeably across sample sizes. In addition, among LNM-informed models, those incorporating both fLNM and sLNM modalities yielded the strongest results. This suggests that both LNM approaches are equally valuable for achieving a high predictive accuracy in general but might also offer complementary information.

Although prediction of almost all cognitive domains was improved by LNM scores, predictive performance for language functions did not exceed that of WMH volumes and confounds (age, sex, and education). From a network perspective, we argue that this finding can be explained by the relatively confined network of left-lateralized brain regions involved in language functions which might present lower vulnerability to WMH disconnectivity compared to cognitive functions such as information processing speed, that rely on a widely distributed network of brain regions.[48] In general, the minor improvement of WMH-based measures over the predictive performance attributed to confounds (age, sex, education) in the whole sample suggests that in this patient population, WMH contribute minimally to the variance in language function.

WMH related to cognitive impairment map to attention control networks

WMH compromise cognitive performance by impacting the function of specific brain networks. To localize these effects, we investigated *regional* associations between functional and structural LNM scores to cognitive performance. We found that higher LNM scores in cortical areas of the dorsal and ventral attention networks were linked to lower attention and executive function, information processing speed and verbal memory (figure 3). Therefore, we infer that higher WMH disconnectivity in these networks is associated with reduced cognitive performance indicating that WMH impair cognitive function by disrupting the respective connecting white matter fiber tracts.

The dorsal attention network – including the frontal eye field, the superior parietal lobule, the intraparietal sulcus and caudal areas of the medial temporal gyrus – governs top-down attention control by enabling voluntary orientation, with increased activity in response to cues indicating the focus location, timing, or subject.[49,50] The ventral attention network comprises the frontal and parietal operculum in the inferior frontal gyrus, medial areas of the

superior frontal cortex and the temporoparietal junction.[42,51] This system exhibits activity increases during bottom-up attention control, i.e., upon detection and orientation to salient targets, especially when they appear in unexpected locations.[49,52] As the effect patterns largely converged on these networks (*supplementary figure S9*), we argue that WMH affect the cognitive functions emerging from these networks, specifically top-down and bottom-up attention control. This aligns with the observation that deficits in attention and executive function are among the most prominent symptoms in CSVD and VCI in general.[1] Furthermore, prior work demonstrates altered resting-state functional connectivity as well as task activation in attention control networks related to CSVD.[53–55] Given the covariance of the identified effect patterns, we speculate that WMH contribute to variance in the performance of other cognitive domains, e.g., information processing speed by affecting the attention demands posited by the corresponding tests.

WMH contribute to cognitive impairment by disrupting frontal and parietal white matter tracts

Regional findings in gray matter areas of the attention control networks are further complemented by white matter tract-level results (figure 4). Functional and structural LNM converged on a significant involvement of tracts connecting frontal and parietal areas involved in attention: the dorsal, medial and ventral section of the superior longitudinal fasciculus – which are known to connect the anterior and posterior parts of the dorsal and ventral attention networks, the medial longitudinal fasciculus, the corticopontine tract, frontoparietal sections of the cingulate, the anterior thalamic radiation, the frontal aslant tract and the arcuate fascicle. Although there were some differences in highlighted tracts between functional and structural LNM, this possibly reflects that both approaches capture different aspects of the same anatomy, with sLNM possibly being more sensitive to direct WMH-induced disruption of axonal connections and functional LNM also reflecting effects mediated via polysynaptic brain circuitry.

Strikingly, in the context of verbal memory, structural WMH disconnectivity pinpointed a distinct set of memory-relevant tracts: the uncinate fascicle, cingulate, and fornix. Intriguingly, disruptions in fornix connectivity due to WMH were associated with improved verbal memory in patients, a finding that appears counterintuitive given the fornix's involvement in maintaining memory function. This paradox may be attributable to WMH disrupting inhibitory fibers. For further discussion covering negative fLNM scores/anticorrelations see *supplementary text S16*.

A unifying hypothesis of WMH disconnectivity

Drawing upon a comprehensive LNM analysis in a memory clinic sample of patients with differing extent and etiology of cognitive impairment, our research converges on a unifying hypothesis: WMH contribute to variance in cognitive functions by disrupting brain circuitry involved in attention control. Our findings not only shed light on the intricate relationships between CSVD, neuroanatomy and cognitive impairment, but they also hint at potential avenues of clinical utilization. The definitive role of CSVD treatments, particularly in precluding cognitive sequelae, is yet to be firmly established. Although there have been promising outcomes related to risk factor modification, particularly blood pressure control,[56,57] pointing towards enhanced cognitive trajectories, clinical trials in VCI require biomarkers to robustly identify vascular contributions to cognitive impairment and vulnerable individuals. Moving forward, leveraging connectivity information could address this gap contributing to patient-tailored therapeutic interventions and facilitating the identification of subgroups at risk of cognitive disorders through vascular lesions likely to reap the most substantial benefits from medical interventions.

Conclusion

WMH-related brain network connectivity measures significantly improve the prediction of current cognitive performance in memory clinic patients compared to WMH volume or epidemiological factors. Our findings highlight the contribution of WMH disconnectivity, particularly in attention-related brain regions, to vascular cognitive impairment. As this research field progresses, harnessing neuroimaging markers of white matter disconnection in CSVD has the potential to aid individualized diagnostic and therapeutic strategies.

Acknowledgements

The authors wish to acknowledge all participants of the Meta VCI Map Consortium. We thank Lei Zhao for his contribution to imaging data harmonization of the Meta VCI Map project data. We thank Guido Cammà and Charlotte M. Verhagen for their contribution to the processing of the imaging data. We thank Olivia K.L. Hamilton, Irene M.C. Huenges Wajer, Bonnie Y.K. Lam, Adrian Wong and Xu Xin as members of the Meta VCI Map neuropsychology working group for their advice on neuropsychological data harmonization.

ADNI data used in preparation of this article were obtained from the Alzheimer's Disease Neuroimaging Initiative (ADNI) database (adni.loni.usc.edu). As such, the investigators within the ADNI contributed to the design and implementation of ADNI and/or provided data but did not participate in analysis or writing of this report. A complete listing of ADNI investigators can be found at: https://adni.loni.usc.edu/wp-content/uploads/how_to_apply/ADNI_Acknowledgement_List.pdf

Funding

This work was funded by the Deutsche Forschungsgemeinschaft (DFG, German Research Foundation – Schwerpunktprogramm 2041 – 454012190 (S.B.E., G.T.); the Meta VCI Map consortium is supported by Vici grant 918.16.616 from ZonMw (G.J.B.) and by Veni grant (project 9150162010055) from ZonMW to JMB; National Institutes of Health (NIH), UCD ADRC NIH awards P30 AG10129 and P30 AG072972 (C.D.); V.V. is supported by JPND-funded E-DADS project (ZonMW project #733051106). ADNI data collection and sharing for this project was funded by the Alzheimer's Disease Neuroimaging Initiative (ADNI) (National Institutes of Health Grant U01 AG024904) and DOD ADNI (Department of Defense award number W81XWH-12-2-0012). ADNI is funded by the National Institute on Aging,

the National Institute of Biomedical Imaging and Bioengineering, and through generous contributions from the following: AbbVie, Alzheimer's Association; Alzheimer's Drug Discovery Foundation; Araclon Biotech; BioClinica, Inc.; Biogen; Bristol-Myers Squibb Company; CereSpir, Inc.; Cogstate; Eisai Inc.; Elan Pharmaceuticals, Inc.; Eli Lilly and Company; EuroImmun; F. Hoffmann-La Roche Ltd and its affiliated company Genentech, Inc.; Fujirebio; GE Healthcare; IXICO Ltd.; Janssen Alzheimer Immunotherapy Research & Development, LLC.; Johnson & Johnson Pharmaceutical Research & Development LLC.; Lumosity; Lundbeck; Merck & Co., Inc.; Meso Scale Diagnostics, LLC.; NeuroRx Research; Neurotrack Technologies; Novartis Pharmaceuticals Corporation; Pfizer Inc.; Piramal Imaging; Servier; Takeda Pharmaceutical Company; and Transition Therapeutics. The Canadian Institutes of Health Research is providing funds to support ADNI clinical sites in Canada. Private sector contributions are facilitated by the Foundation for the National Institutes of Health (www.fnih.org). The grantee organization is the Northern California Institute for Research and Education, and the study is coordinated by the Alzheimer's Therapeutic Research Institute at the University of Southern California. ADNI data are disseminated by the Laboratory for Neuro Imaging at the University of Southern California.

Competing interests

GT has received fees as consultant or lecturer from Acandis, Alexion, Amarin, Bayer, Boehringer Ingelheim, BristolMyersSquibb/Pfizer, Daichi Sankyo, Portola, and Stryker outside the submitted work.

References

1. Dichgans Martin, Leys Didier. Vascular Cognitive Impairment. *Circulation Research*. 2017;120(3):573-591. doi:10.1161/CIRCRESAHA.116.308426
2. Wardlaw JM, Smith EE, Biessels GJ, et al. Neuroimaging standards for research into small vessel disease and its contribution to ageing and neurodegeneration. *The Lancet Neurology*. 2013;12(8):822-838. doi:10.1016/S1474-4422(13)70124-8
3. Duering M, Biessels GJ, Brodtmann A, et al. Neuroimaging standards for research into small vessel disease—advances since 2013. *The Lancet Neurology*. Published online May 23, 2023. doi:10.1016/S1474-4422(23)00131-X
4. Biesbroek JM, Weaver NA, Hilal S, et al. Impact of Strategically Located White Matter Hyperintensities on Cognition in Memory Clinic Patients with Small Vessel Disease. *PLOS ONE*. 2016;11(11):e0166261. doi:10.1371/journal.pone.0166261
5. Kloppenborg RP, Nederkoorn PJ, Geerlings MI, van den Berg E. Presence and progression of white matter hyperintensities and cognition: a meta-analysis. *Neurology*. 2014;82(23):2127-2138. doi:10.1212/WNL.0000000000000505
6. Coenen M, Kuijf HJ, Huenges Wajer IMC, et al. Strategic white matter hyperintensity locations for cognitive impairment: A multicenter lesion-symptom mapping study in 3525 memory clinic patients. *Alzheimer's & Dementia*. Published online December 12, 2022:alz.12827. doi:10.1002/alz.12827
7. Duering M, Gesierich B, Seiler S, et al. Strategic white matter tracts for processing speed deficits in age-related small vessel disease. *Neurology*. 2014;82(22):1946-1950. doi:10.1212/WNL.0000000000000475
8. ter Telgte A, van Leijsen EMC, Wiegertjes K, Klijn CJM, Tuladhar AM, de Leeuw FE. Cerebral small vessel disease: from a focal to a global perspective. *Nature Reviews Neurology*. 2018;14(7):387-398. doi:10.1038/s41582-018-0014-y
9. Salvalaggio A, De Filippo De Grazia M, Zorzi M, Thiebaut de Schotten M, Corbetta M. Post-stroke deficit prediction from lesion and indirect structural and functional disconnection. *Brain*. 2020;143(7):2173-2188. doi:10.1093/brain/awaa156
10. Foulon C, Cerliani L, Kinkingnéhun S, et al. Advanced lesion symptom mapping analyses and implementation as BCBtoolkit. *Gigascience*. 2018;7(3):1-17. doi:10.1093/gigascience/giy004
11. Talozzi L, Forkel SJ, Pacella V, et al. Latent disconnectome prediction of long-term cognitive-behavioural symptoms in stroke. *Brain*. Published online March 16, 2023:awad013. doi:10.1093/brain/awad013
12. Siddiqi SH, Kletenik I, Anderson MC, et al. Lesion network localization of depression in multiple sclerosis. *Nat Mental Health*. 2023;1(1):36-44. doi:10.1038/s44220-022-00002-y
13. Weaver NA, Zhao L, Biesbroek JM, et al. The Meta VCI Map consortium for meta-analyses on strategic lesion locations for vascular cognitive impairment using lesion-symptom mapping: Design and multicenter pilot study. *Alzheimers Dement (Amst)*. 2019;11:310-326. doi:10.1016/j.dadm.2019.02.007
14. Jack CR, Barnes J, Bernstein MA, et al. Magnetic resonance imaging in Alzheimer's Disease Neuroimaging Initiative 2. *Alzheimers Dement*. 2015;11(7):740-756. doi:10.1016/j.jalz.2015.05.002
15. Hinton L, Carter K, Reed BR, et al. Recruitment of a community-based cohort for research on diversity and risk of dementia. *Alzheimer Dis Assoc Disord*. 2010;24(3):234-241. doi:10.1097/WAD.0b013e3181c1ee01
16. Case NF, Charlton A, Zwiers A, et al. Cerebral Amyloid Angiopathy Is Associated With Executive Dysfunction and Mild Cognitive Impairment. *Stroke*. 2016;47(8):2010-2016. doi:10.1161/STROKEAHA.116.012999
17. Pusswald G, Lehrner J, Hagmann M, et al. Gender-Specific Differences in Cognitive Profiles of Patients with Alzheimer's Disease: Results of the Prospective Dementia Registry Austria (PRODEM-Austria). *J Alzheimers Dis*. 2015;46(3):631-637. doi:10.3233/JAD-150188
18. Boomsma JMF, Exalto LG, Barkhof F, et al. Vascular Cognitive Impairment in a Memory Clinic Population: Rationale and Design of the "Utrecht-Amsterdam Clinical Features and Prognosis in Vascular Cognitive Impairment" (TRACE-VCI) Study. *JMIR Res Protoc*. 2017;6(4):e60. doi:10.2196/resprot.6864
19. Weaver NA, Kuijf HJ, Aben HP, et al. Strategic infarct locations for post-stroke cognitive impairment: a pooled analysis of individual patient data from 12 acute ischaemic stroke cohorts. *The Lancet Neurology*. 2021;0(0). doi:10.1016/S1474-4422(21)00060-0
20. Kuijf HJ, Biesbroek JM, De Bresser J, et al. Standardized Assessment of Automatic Segmentation of White Matter Hyperintensities and Results of the WMH Segmentation Challenge. *IEEE Trans Med Imaging*. 2019;38(11):2556-2568. doi:10.1109/TMI.2019.2905770
21. Biesbroek JM, Kuijf HJ, Weaver NA, et al. Brain Infarct Segmentation and Registration on MRI or CT for Lesion-symptom Mapping. *J Vis Exp*. 2019;(151). doi:10.3791/59653
22. Yeh FC. Population-based tract-to-region connectome of the human brain and its hierarchical topology. *Nat Commun*. 2022;13(1):4933. doi:10.1038/s41467-022-32595-4
23. Coenen M, Biessels GJ, DeCarli C, et al. Spatial distributions of white matter hyperintensities on brain MRI: A pooled analysis of individual participant data from 11 memory clinic cohorts. *NeuroImage: Clinical*. 2023;40:103547. doi:10.1016/j.nicl.2023.103547
24. Jiang J, Bruss J, Lee WT, Tranel D, Boes AD. White matter disconnection of left multiple demand network is associated with post-lesion deficits in cognitive control. *Nat Commun*. 2023;14(1):1740. doi:10.1038/s41467-023-37330-1
25. Schaefer A, Kong R, Gordon EM, et al. Local-Global Parcellation of the Human Cerebral Cortex from Intrinsic Functional Connectivity MRI. *Cerebral Cortex*. 2018;28(9):3095-3114. doi:10.1093/cercor/bhx179
26. Tian Y, Margulies DS, Breakspear M, Zalesky A. Topographic organization of the human subcortex unveiled with functional connectivity gradients. *Nat Neurosci*. 2020;23(11):1421-1432. doi:10.1038/s41593-020-00711-6
27. Cohen A, Soussand L, McManus P, Fox M. GSP1000 Preprocessed Connectome. Published online April 17, 2021. doi:10.7910/DVN/ILXIKS
28. Yeo BTT, Krienen FM, Sepulcre J, et al. The organization of the human cerebral cortex estimated by intrinsic functional connectivity. *J Neurophysiol*. 2011;106(3):1125-1165. doi:10.1152/jn.00338.2011
29. Neudorfer C, Butenko K, Oxenford S, et al. Lead-DBS v3.0: Mapping deep brain stimulation effects to local anatomy and global networks.

NeuroImage. 2023;268:119862. doi:10.1016/j.neuroimage.2023.119862
30. Horn A, Reich M, Vorwerk J, et al. Connectivity Predicts deep brain stimulation outcome in Parkinson disease. *Annals of Neurology*. 2017;82(1):67-78. doi:10.1002/ana.24974
31. Fang-Cheng Yeh, Wedeen VJ, Tseng WYI. Generalized q-Sampling Imaging. *IEEE Trans Med Imaging*. 2010;29(9):1626-1635. doi:10.1109/TMI.2010.2045126
32. Hamdan S, More S, Sasse L, et al. Julearn: an easy-to-use library for leakage-free evaluation and inspection of ML models. *Gigabyte*. 2024;2024:1-16. doi:10.46471/gigabyte.113
33. Abraham A, Pedregosa F, Eickenberg M, et al. Machine learning for neuroimaging with scikit-learn. *Frontiers in Neuroinformatics*. 2014;8. Accessed March 28, 2022. https://www.frontiersin.org/article/10.3389/fninf.2014.00014
34. Poldrack RA, Huckins G, Varoquaux G. Establishment of Best Practices for Evidence for Prediction: A Review. *JAMA Psychiatry*. 2020;77(5):534-540. doi:10.1001/jamapsychiatry.2019.3671
35. Omidvarnia A, Sasse L, Larabi DI, et al. Is resting state fMRI better than individual characteristics at predicting cognition? Published online April 25, 2023:2023.02.18.529076. doi:10.1101/2023.02.18.529076
36. Varoquaux G, Raamana PR, Engemann DA, Hoyos-Idrobo A, Schwartz Y, Thirion B. Assessing and tuning brain decoders: Cross-validation, caveats, and guidelines. *NeuroImage*. 2017;145:166-179. doi:10.1016/j.neuroimage.2016.10.038
37. Nadeau C, Bengio Y. Inference for the Generalization Error. *Machine Learning*. 2003;52(3):239-281. doi:10.1023/A:1024068626366
38. Vallat R. Pingouin: statistics in Python. *JOSS*. 2018;3(31):1026. doi:10.21105/joss.01026
39. Winkler AM, Ridgway GR, Webster MA, Smith SM, Nichols TE. Permutation inference for the general linear model. *Neuroimage*. 2014;92:381-397. doi:10.1016/j.neuroimage.2014.01.060
40. Markello RD, Hansen JY, Liu ZQ, et al. neuromaps: structural and functional interpretation of brain maps. *Nat Methods*. Published online October 6, 2022:1-8. doi:10.1038/s41592-022-01625-w
41. Margulies DS, Ghosh SS, Goulas A, et al. Situating the default-mode network along a principal gradient of macroscale cortical organization. *Proc Natl Acad Sci U S A*. 2016;113(44):12574-12579. doi:10.1073/pnas.1608282113
42. Fox MD, Snyder AZ, Vincent JL, Corbetta M, Van Essen DC, Raichle ME. The human brain is intrinsically organized into dynamic, anticorrelated functional networks. *Proceedings of the National Academy of Sciences*. 2005;102(27):9673-9678. doi:10.1073/pnas.0504136102
43. Fox MD, Zhang D, Snyder AZ, Raichle ME. The Global Signal and Observed Anticorrelated Resting State Brain Networks. *Journal of Neurophysiology*. 2009;101(6):3270-3283. doi:10.1152/jn.90777.2008
44. De Luca A, Kuijf H, Exalto L, Thiebaut de Schotten M, Biessels GJ. Multimodal tract-based MRI metrics outperform whole brain markers in determining cognitive impact of small vessel disease-related brain injury. *Brain Struct Funct*. 2022;227(7):2553-2567. doi:10.1007/s00429-022-02546-2
45. Frey BM, Petersen M, Schlemm E, et al. White matter integrity and structural brain network topology in cerebral small vessel disease: The Hamburg city health study. *Hum Brain Mapp*. 2021;42(5):1406-1415. doi:10.1002/hbm.25301
46. Schlemm E, Frey BM, Mayer C, et al. Equalization of Brain State Occupancy Accompanies Cognitive Impairment in Cerebral Small Vessel Disease. *Biological Psychiatry*. 2022;92(7):592-602. doi:10.1016/j.biopsych.2022.03.019
47. Pini L, Salvalaggio A, De Filippo De Grazia M, Zorzi M, Thiebaut de Schotten M, Corbetta M. A novel stroke lesion network mapping approach: improved accuracy yet still low deficit prediction. *Brain Communications*. 2021;3(4):fcab259. doi:10.1093/braincomms/fcab259
48. Friederici AD. The Brain Basis of Language Processing: From Structure to Function. *Physiological Reviews*. 2011;91(4):1357-1392. doi:10.1152/physrev.00006.2011
49. Corbetta M, Kincade JM, Ollinger JM, McAvoy MP, Shulman GL. Voluntary orienting is dissociated from target detection in human posterior parietal cortex. *Nat Neurosci*. 2000;3(3):292-297. doi:10.1038/73009
50. Shulman GL, McAvoy MP, Cowan MC, et al. Quantitative analysis of attention and detection signals during visual search. *J Neurophysiol*. 2003;90(5):3384-3397. doi:10.1152/jn.00343.2003
51. Alves PN, Forkel SJ, Corbetta M, Thiebaut de Schotten M. The subcortical and neurochemical organization of the ventral and dorsal attention networks. *Commun Biol*. 2022;5(1):1-14. doi:10.1038/s42003-022-04281-0
52. Astafiev SV, Shulman GL, Stanley CM, Snyder AZ, Van Essen DC, Corbetta M. Functional organization of human intraparietal and frontal cortex for attending, looking, and pointing. *J Neurosci*. 2003;23(11):4689-4699. doi:10.1523/JNEUROSCI.23-11-04689.2003
53. Schulz M, Malherbe C, Cheng B, Thomalla G, Schlemm E. Functional connectivity changes in cerebral small vessel disease - a systematic review of the resting-state MRI literature. *BMC Med*. 2021;19:103. doi:10.1186/s12916-021-01962-1
54. Ding JR, Ding X, Hua B, et al. Altered connectivity patterns among resting state networks in patients with ischemic white matter lesions. *Brain Imaging Behav*. 2018;12(5):1239-1250. doi:10.1007/s11682-017-9793-9
55. Dey AK, Stamenova V, Turner G, Black SE, Levine B. Pathoconnectomics of cognitive impairment in small vessel disease: A systematic review. *Alzheimer's & Dementia*. 2016;12(7):831-845. doi:10.1016/j.jalz.2016.01.007
56. SPRINT MIND Investigators for the SPRINT Research Group, Williamson JD, Pajewski NM, et al. Effect of Intensive vs Standard Blood Pressure Control on Probable Dementia: A Randomized Clinical Trial. *JAMA*. 2019;321(6):553-561. doi:10.1001/jama.2018.21442
57. Veronese N, Facchini S, Stubbs B, et al. Weight loss is associated with improvements in cognitive function among overweight and obese people: A systematic review and meta-analysis. *Neuroscience & Biobehavioral Reviews*. 2017;72:87-94. doi:10.1016/j.neubiorev.2016.11.017

Table 1. Sample characteristics

Metric	*Stat*
Age in years, mean ± SD (n)	71.71 ± 8.87 (3485)
Female, n (%)	1737 (49.8)
Years of education, mean ± SD (n)	12.89 ± 4.45 (3485)
Patient ethnicity	
Afrocaribbean, n (%)	198 (5.7)
Asian, n (%)	237 (6.8)
Caucasian / European / White, n (%)	1620 (46.5)
Hispanic, n (%)	146 (4.2)
Other, n (%)	52 (1.5)
Diagnosis	
Subjective cognitive impairment	777 (22.30)
Mild cognitive impairment	1389 (39.86)
Dementia	1319 (37.85)
For dementia cases: probable etiology	
Alzheimer's dementia, n (%)	764 (57.9)
Vascular dementia, n (%)	85 (6.4)
Frontotemporal dementia, n (%)	44 (3.3)
Dementia with Lewy bodies, n (%)	24 (1.8)
Cardiovascular risk factors	
Current smoking, n (%)	499 (14.3)
Previous smoking, n (%)	459 (13.2)
Hypertension, n (%)	1714 (49.2)
Hypercholesterolemia, n (%)	1098 (31.5)
Diabetes mellitus, n (%)	492 (14.1)
BMI, mean ± SD (n)	25.28 ± 4.75 (640)
Comorbidities	
Atrial fibrillation, n (%)	98 (2.8)
History of prior stroke, n (%)	244 (7.0)
History of prior transient ischemic attack (TIA), n (%)	62 (1.8)
History of prior other vascular events, n (%)	715 (20.5)
Imaging	
WMH volume in ml, median [IQR] (n)	6.19 [14.21] (3485)
Cognitive function	
Mini-mental state examination, mean ± SD (n)	25.0 ± 4.7 (3327)
Attention / executive function, z, mean ± SD (n)	-1.12 ± 1.10 (3446)
Information processing speed, z, mean ± SD (n)	-0.96 ± 1.61 (2417)
Language, z, mean ± SD (n)	-1.08 ± 1.86 (2041)
Verbal memory, z, mean ± SD (n)	-1.48 ± 1.30 (3242)

Abbreviations: ml = milliliter, SD – standard deviation, z – harmonized z-score

a) Data
Meta VCI Map Consortium
($n_{cohorts}$=10, $n_{patients}$=3485)
TRACE-VCI
UMCC
AGE
VASCAMY
PRODEM
FAVR
Brain'IMPACT
ADNI
AUCD
Harmonization
Functional connectome
rsfMRI - GSP1000
Structural connectome
Tractography - HCP32
Cognitive data
WMH segmentations
2D
3D
b) Lesion network mapping
Schaefer400x7 Atlas
n_{ROIs}=400
Melbourne Subcort. Atlas
n_{ROIs}=16
HCP1065 Tract Atlas
n_{ROIs}=64
Region of interest (ROI)
Correlated
Anticorrelated
WMH
Functional connectivity map
Functional WMH connectivity
fLNM scores
$n_{patients}$
n_{ROIs}
Structural connectivity map
Structural WMH connectivity
sLNM scores
c) Analyses
Predictive modelling analysis
Region of interest analysis
Tract 5
Tract 6
Tract 4
Tract 7
Tract 3
Tract 8
Tract 2
Tract 1
0.2
0.1
0
−0.1
−0.2
β

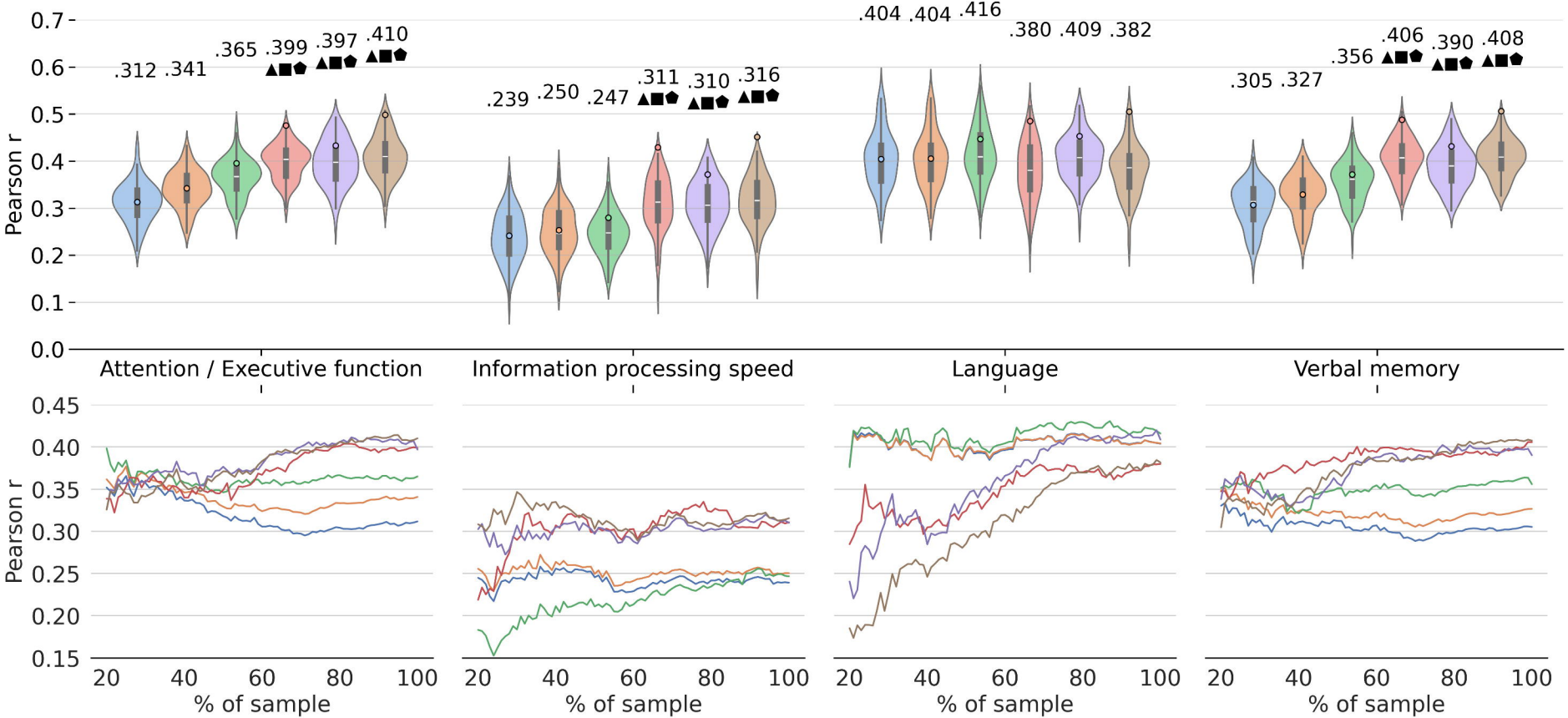

Features

- Confounds (age, sex and education)
- WMH volume + confounds
- Tract-level WMH volumes + confounds
- sLNM + confounds
- fLNM + confounds
- sLNM + fLNM + confounds

o : Train score average

t – test comparisons

▲: >Confounds

■: >WMH volume + confounds

⬟: >Tract-level WMH volumes + confounds

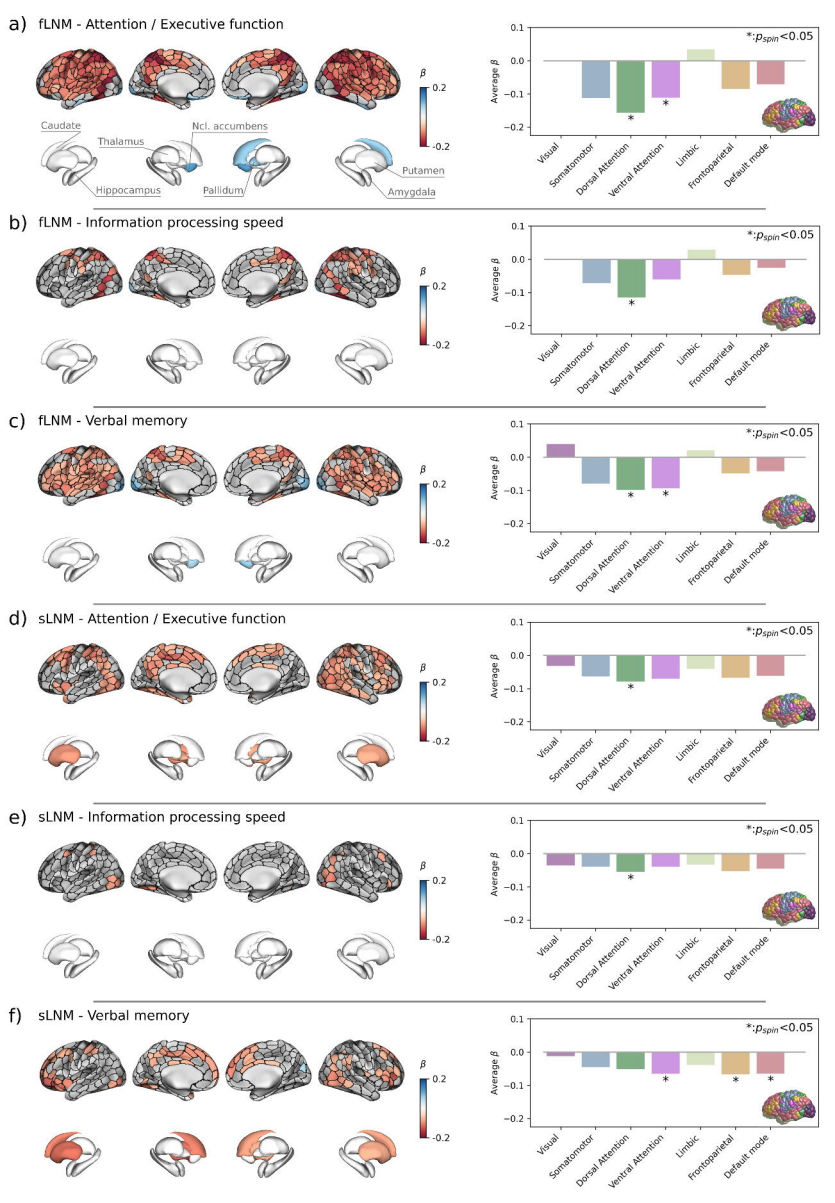
a) fLNM - Attention / Executive function
Caudate
Thalamus
Ncl. accumbens
Hippocampus
Pallidum
Putamen
Amygdala
β
0.2
-0.2
*:p_{spin}<0.05
Average β
0.1
0.0
-0.1
-0.2
Visual
Somatomotor
Dorsal Attention
Ventral Attention
Limbic
Frontoparietal
Default mode
b) fLNM - Information processing speed
c) fLNM - Verbal memory
d) sLNM - Attention / Executive function
e) sLNM - Information processing speed
f) sLNM - Verbal memory

a)

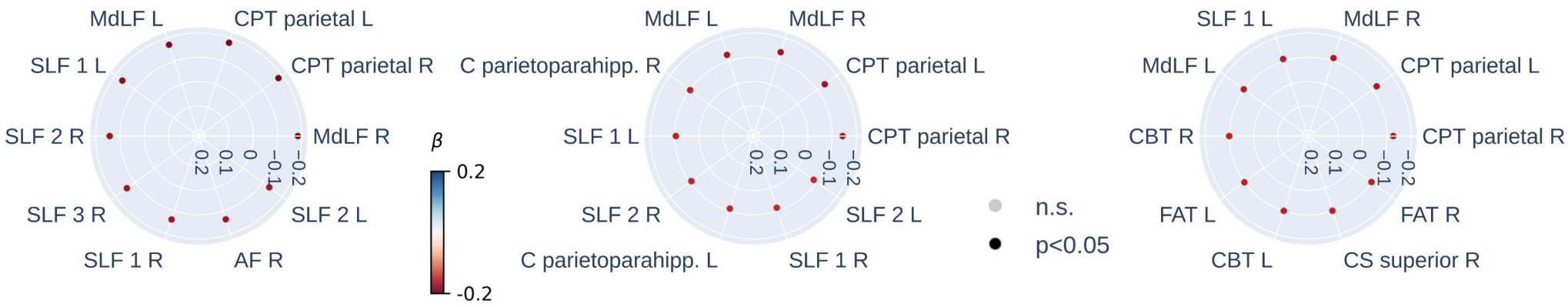

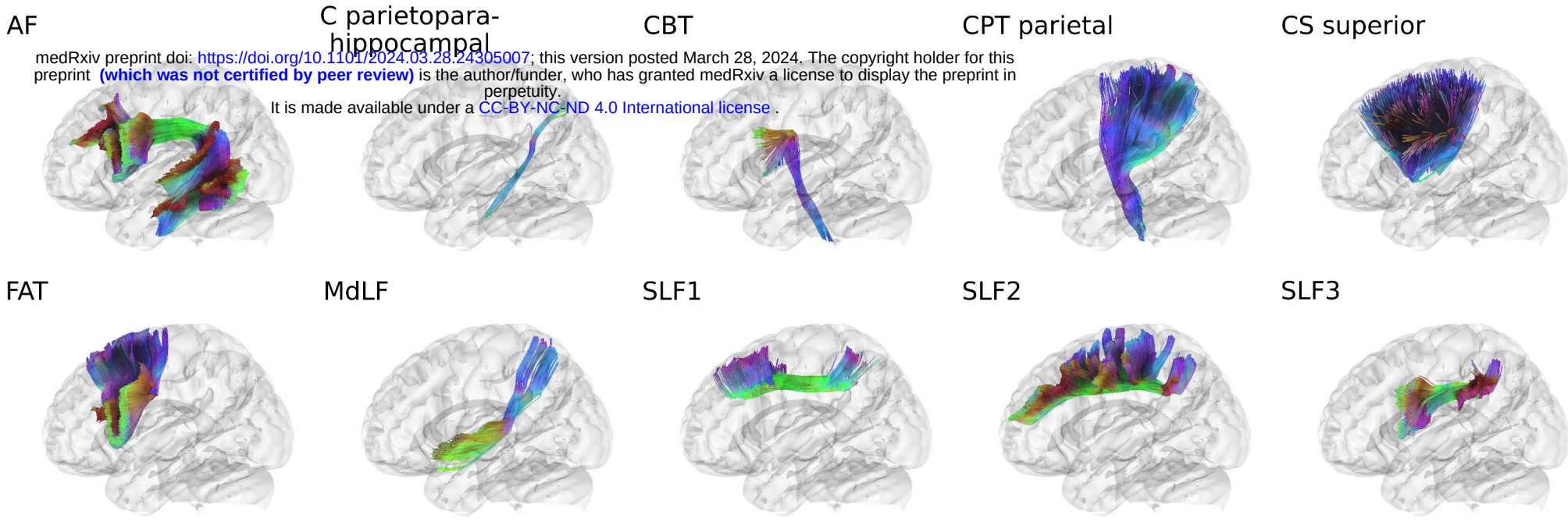

b)